Cell Reports, Volume *31*

Supplemental Information

Chaperone-Mediated Protein Disaggregation Triggers Proteolytic Clearance of Intra-nuclear Protein Inclusions

Fabian den Brave, Lucas V. Cairo, Chandhuru Jagadeesan, Carmen Ruger-Herreros, Axel Mogk, Bernd Bukau, and Stefan Jentsch

Figure S1 (related to Figure 1)

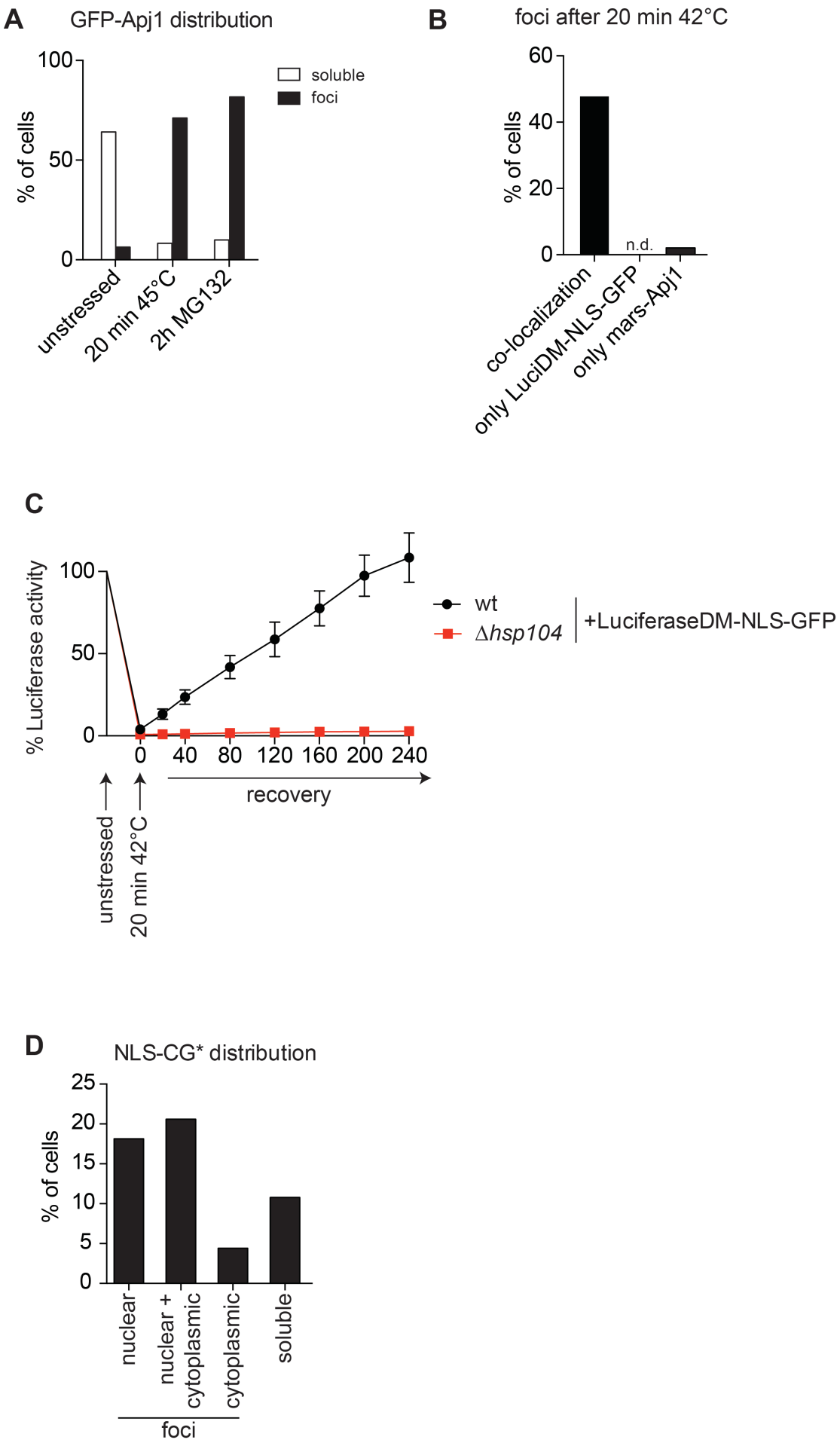

Figure S1. Apj1 is recruited to nuclear protein inclusions (related to Figure 1) (A) Distribution of Apj1 in response to stress. Quantification of Apj1 distribution described in (1A). For each condition at least 200 cells were counted. Total number of cells is set to 100 %. **(B)** Co-localization of Apj1 and nuclear Luciferase. Quantification of cells described in (1B). Nuclear foci being only GFP-positive (only LuciDM-NLS-GFP), only mars positive (only mars-Apj1) or showing both fluorescent signals (co-localization) were counted. Approximately 300 cells were counted. Total number of cells is set to 100 %. **(C)** In vivo Luciferase disaggregation assay. The indicated strains expressing LuciDM-NLS as in were subjected to 42°C for 20 min to aggregate nuclear Luciferase. Disaggregation was determined by measuring Luciferase activity at different time-points after heatshock as indicated. Luciferase activity measured before heatshock was set to 100 %. Quantification shows averages ± SD from three independent experiments. **(D)** Subcellular distribution of NLS-CG*. Quantification of NLS-CG* distribution in cells as shown in (1F). Distribution of NLS-CG* was analyzed in more than 200 cells. Total number of cells is set to 100 %.

Figure S2 (related to Figure 2)

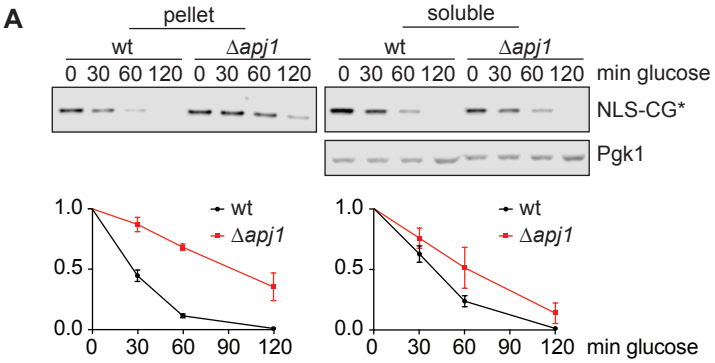

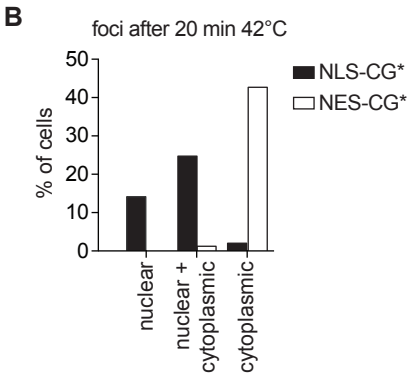

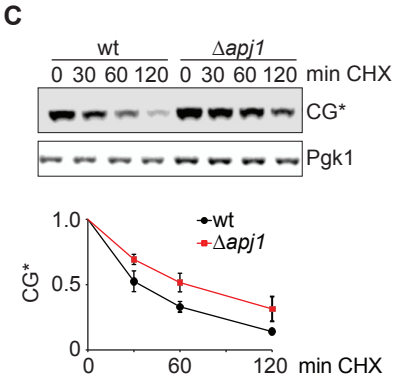

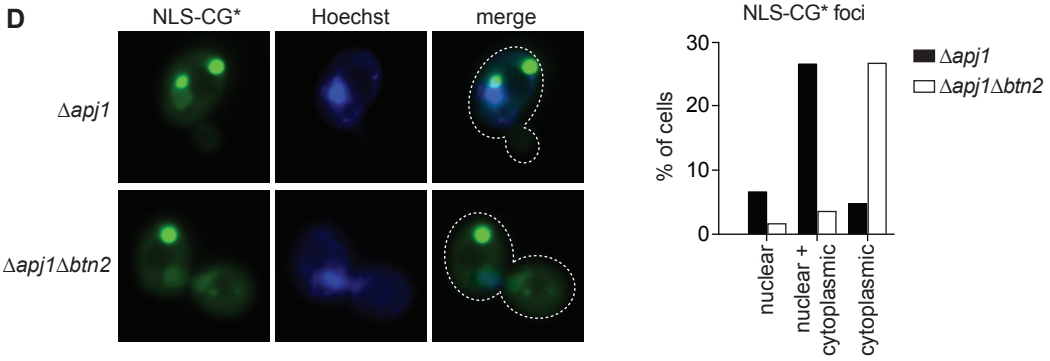

Figure S2. Role of nuclear protein aggregation on Apj1 dependent turnover (related to Figure 2). (A) Apj1-dependent turnover of soluble and insoluble NLS-CG* without cycloheximide addition. Degradation of NLS-CG* was followed after addition of glucose. Samples of each time point were fractionated as in (2A). NLS-CG* was detected using anti-GFP antibodies. Soluble Pgk1 serves as a control. Quantification below shows averages ± SD from three independent experiments. **(B)** Subcellular distribution of NLS/NES-CG*. Quantification of NLS-CG* and NES-CG* foci following acute heat stress as in (2C). Around 80 cells were counted for NLS-CG* and about 200 for NES-CG*. Total number of cells is set to 100 %. **(C)** Effect of Apj1 on turnover of CG* without additional targeting signal. Turnover of CG* was analyzed in the indicated strains as in (1G). Quantification shows averages ± SD from three independent experiments. **(D)** Effect of Btn2 on the distribution of NLS-CG*. NLS-CG* was expressed in the indicated strains. NLS-CG* distribution was analyzed by live cell imaging. Nuclei were counterstained with Hoechst. Dashed lines indicate position of nucleus. Quantification shows NLS-CG* foci distribution from more than 200 cells for each strain. Total number of cells is set to 100 %.

Figure S3 (related to Figure 3)

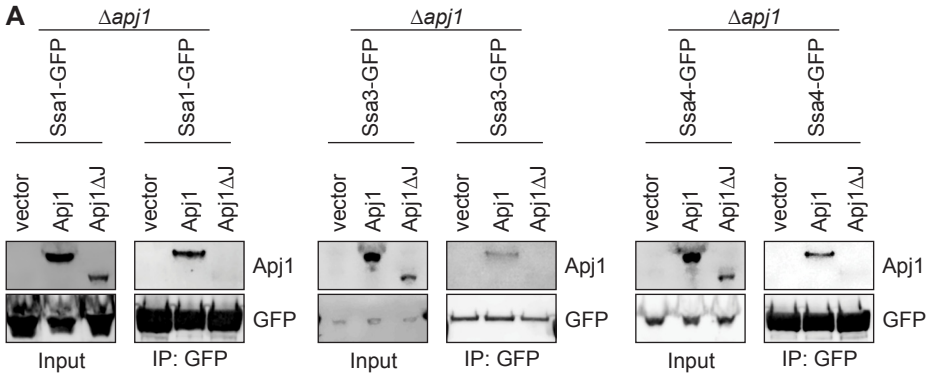

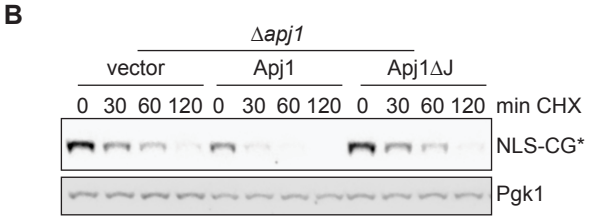

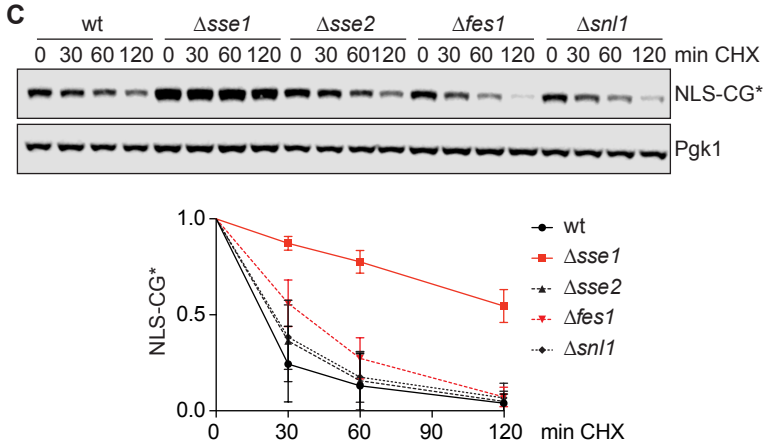

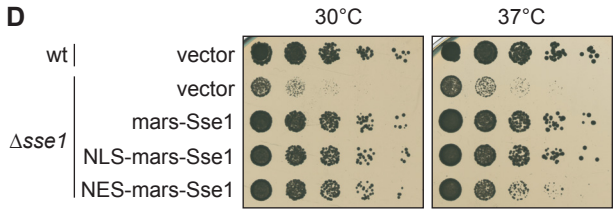

Figure S3. Role of Hsp70 machinery in Apj1 dependent protein aggregate clearance (related to Figure 3). (A) Interaction of Apj1 with Hsp70. Genomically tagged Hsp70 (Ssa1, Ssa3, Ssa4) were co-expressed with the indicated Apj1 variants or empty vector. Hsp70-Apj1 interaction was assessed by GFP-pulldowns as in (3B). Binding proteins were analyzed by westernblotting using GFP and Apj1 specific antibodies. IP, immunoprecipitation. **(B)** Role of Hsp70 interaction in Apj1 dependent degradation. NLS-CG* turnover was analyzed in *Δapj1* cells expressing the indicated Apj1 variants or the corresponding empty vector as described in (1G). **(C)** Role of Hsp70 NEFs on NLS-CG* degradation. Indicated strains were analyzed as in (1G). Quantification shows averages ± SD from three independent experiments. **(D)** Complementation of Sse1 deficient cells by differentially localized Sse1 variants. Empty vector or the indicated Sse1 variants were expressed in the indicated strains. 5 times serial dilutions of the indicated yeast were spotted onto YPD plates and incubated at the indicated temperatures.

Figure S4 (related to Figure 4)

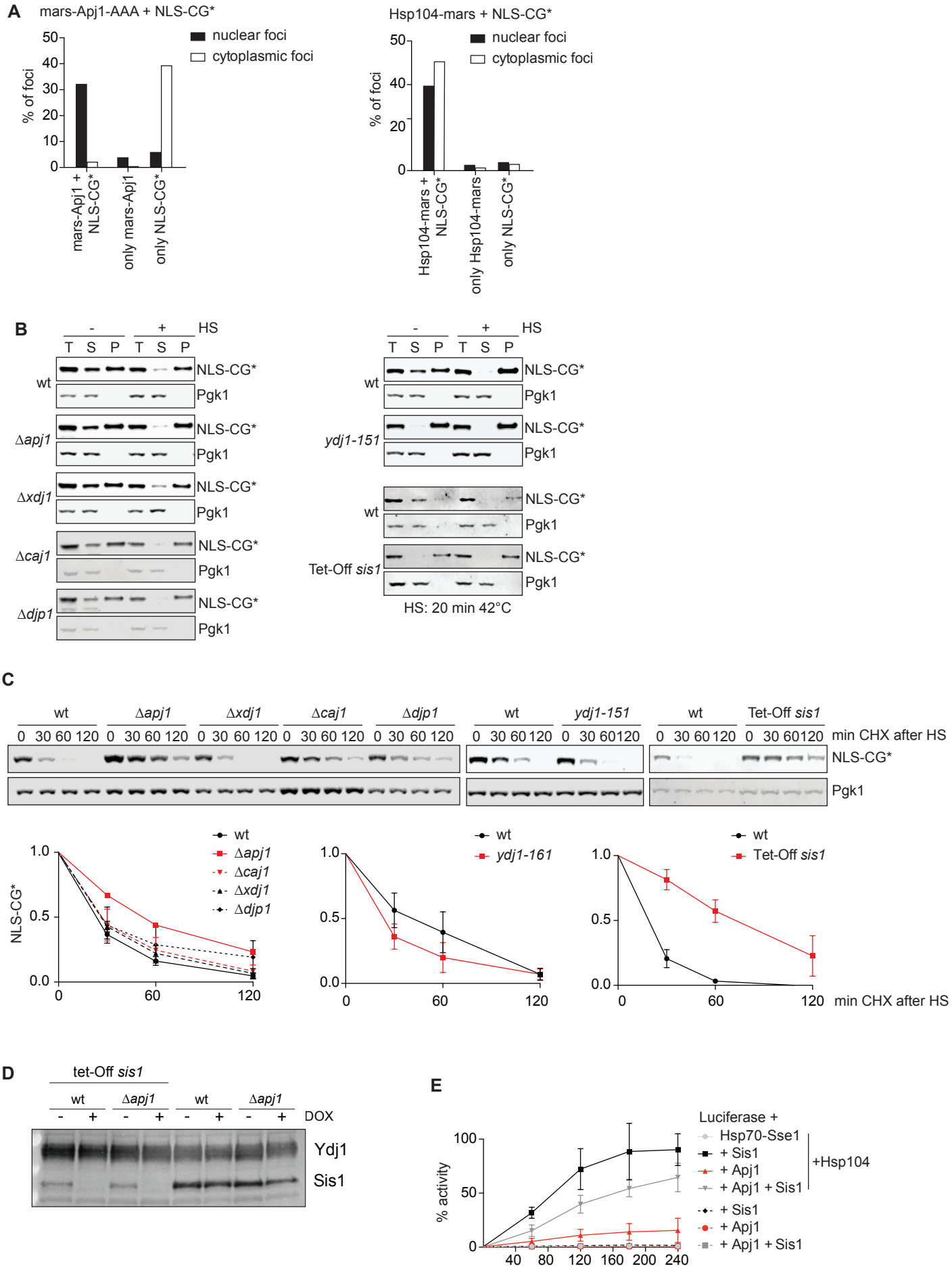

Figure S4. Role of J-proteins on NLS-CG* solubility and turnover (related to Figure 4). (A) Co-localization of Apj1 and Hsp104 with NLS-CG*. Related to (4B). Nuclear and cytoplasmic foci were analyzed for NLS-CG* and mars-Apj1 or Hsp104-mars content, respectively. More than 200 foci were counted. Total number of foci is set to 100 %. **(B)** Impact of Hsp40 chaperones on NLS-CG* solubility. The indicated strains expressing NLS-CG* were left unstressed or subjected to acute heat stress and analyzed as in (2A). Sis1 was depleted by addition of Dox. **(C)** Impact of Hsp40 chaperones on NLS-CG* turnover. The stability of NLS-CG* was analyzed in the indicated strains as described in (1G). For Sis1 depletion, cells were grown in presence of Dox. Quantification shows averages ± SD from three independent experiments. **(D)** Analysis of Sis1 depletion. Sis1 levels of the indicated strains grown in presence (+) or absence (-) of Dox were analyzed by westernblotting using Sis1 specific antibodies. Ydj1 serves as loading control. **(E).** Role of different chaperones in Luciferase disaggregation and refolding in vitro. Luciferase was aggregated at 42°C for 20 min. Luciferase activitiy was determined at different time points during incubation at 30°C in presence of the indicated chaperones and an ATP regenerating system. The activity of native Luciferase was set as 100 %. Averages ± SD from three independent experiments are shown.

Figure S5 (related to Figure 5)

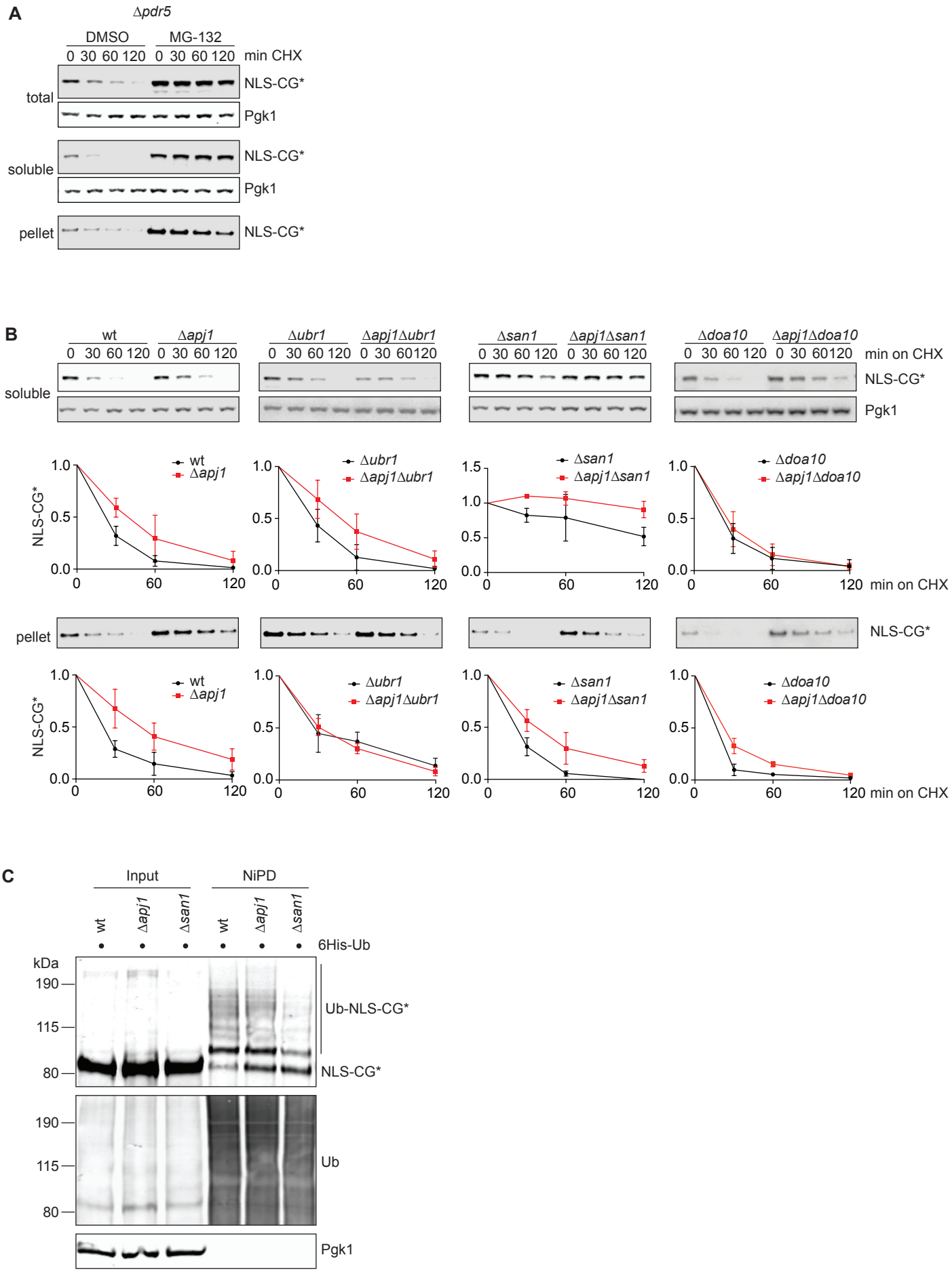

Figure S5. Role of the ubiquitin proteasome system in NLS-CG* turnover (related to Figure 5). (A) Impact of proteasome inhibition on the stability of soluble and insoluble NLS-CG*. Stability of soluble and insoluble NLS-CG* was analyzed as in (2B) in an otherwise wild-type strain lacking Pdr5 and in absence or presence of MG-132. **(B)** Impact of individual nuclear ubiquitin ligases on NLS-CG* turnover. Degradation of soluble and insoluble NLS-CG* in the indicated strains was analyzed as in (2B). Averages ± SD from three independent experiments are shown. **(C)** Impact of Apj1 on NLS-CG* ubiquitylation. NLS-CG* was co-expressed with 6His-Ubiquitin in the indicated strains. Ubiquitin conjugates were purified under denaturing conditions using Ni-pulldown. Ubiquitiylated NLS-CG* in the pulldown was identified by western blotting using GFP antibodies. Ubiquitin specific antibodies serve as pulldown control, Pgk1 serves as loading control of the input fraction. Ub-NLS-CG* denotes ubiquitin modified NLS-CG*; NiPD: Ni-pulldown.

Figure S6 (related to Figure 6)

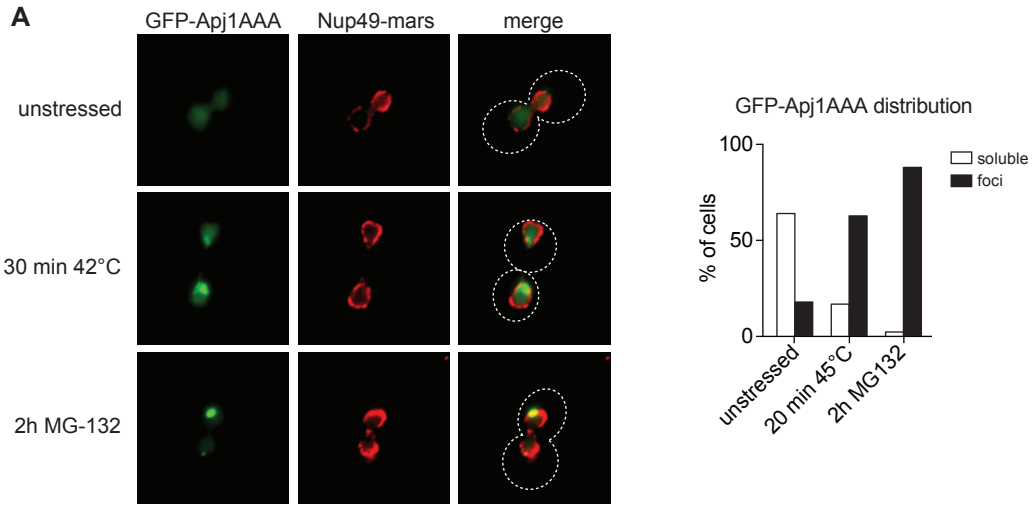

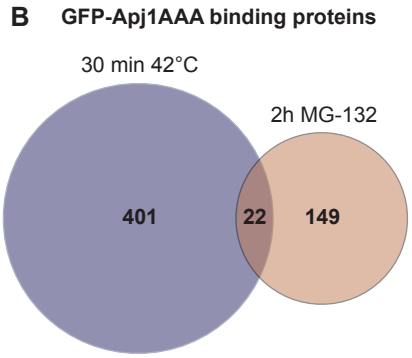

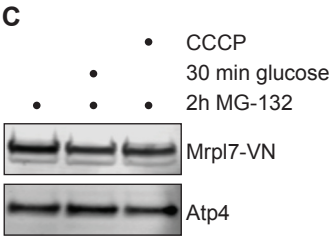

Supplementary table 2

Plasmids used in this study

name	plasmid	reference
pFA0026	prs315	(Sikorski and Hieter, 1989)
pFA0825	prs315 pApj1 GFP-Apj1	this study
pFA0876	prs315 pApj1 GFP-Apj1AAA	this study
pFA0379	pcu426 LuciDM-NLS-GFP	this study
pFA0762	pcu426 pGAL1 NLS-CG*	this study
pFA0765	p413 pGAL1 CG*	(Park et al., 2013)
pFA0766	p413 pGAL1 NLS-CG*	(Park et al., 2013)
pFA0872	p413 pGAL1 NES-CG*	(Park et al., 2013)
pFA0824	prs315 pApj1 Apj1	this study
pFA0809	prs315 pApj1 Apj1AAA	this study
pFA0875	prs315 pApj1 mars-Apj1AAA	this study
pFA1024	prs315 pAPJ1 VC-Apj1	this study
pFA1025	p413 pGAL1 Cse4-VN	this study
pFA1026	p413 pGAL1 Mrpl7-VN	this study
pFA1033	p413 pGAL1 Pgk1-VN	this study
pFA1034	p413 pGAL1 Orc4-VN	this study
pFA0173	p415	(Mumberg et al., 1995)
pFA1027	p415 pSSE1 mars-Sse1	this study
pFA1029	p415 pSSE1 NLS-mars-Sse1	this study
pFA1031	p415 pSSE1 NES-mars-Sse1	this study
pFA1040	pADH 8His-Ubiquitin	M. Glickman

Mumberg, D., R. Muller, and M. Funk. 1995. Yeast vectors for the controlled expression of heterologous proteins in different genetic backgrounds. *Gene*. 156:119-122.

Park, S.H., Y. Kukushkin, R. Gupta, T. Chen, A. Konagai, M.S. Hipp, M. Hayer-Hartl, and F.U. Hartl. 2013. PolyQ proteins interfere with nuclear degradation of cytosolic proteins by sequestering the Sis1p chaperone. *Cell*. 154:134-145.

Sikorski, R.S., and P. Hieter. 1989. A system of shuttle vectors and yeast host strains designed for efficient manipulation of DNA in Saccharomyces cerevisiae. *Genetics*. 122:19-27.

Supplementary table 3

Strains used in this study

name	relevant genotype	background	reference
yFA1791	*his3Δ1, leu2Δ0, lys2Δ0, ura3Δ0*	S288c	*http://www.euroscarf.de*
yFA3566	*Δapj1::NatNT2, Δpdr5::hphNT2*	S288c	*this study*
yFA2251	*Nup49-mars::KanMX6*	S288c	*this study*
yFA1837	*Δapj1::NatNT2*	S288c	*this study*
yFA2249	*Δapj1::NatNT2, Nup49-mars::KanMX6*	S288c	*this study*
yFA1913	*Δbtn2::NatNT2*	S288c	*this study*
yFA3222	*Δapj1::hphNT2, Δbtn2::NatNT2*	S288c	*this study*
yFA2082	*Δhsp42::KanMX, Δbtn2::NatNt2*	S288c	*this study*
yFA3207	*Δapj1::hphNT2, Δbtn2::NatNt2, Δhsp42::KanMX,*	S288c	*this study*
yFA3258	*Δhsp104::KanMX6*	S288c	*this study*
yFA3325	*Δapj1::NatNT2, Δhsp104::KanMX6*	S288c	*this study*
yFA3887	*Hsp104-mars::KanMX6*	S288c	*this study*
yFA3889	*Δapj1::NatNT2, Hsp104-mars::KanMX6*	S288c	*this study*
yFA1890	*Δsse1::hphNT2*	S288c	*this study*
yFA2161	*Δsse2::kanMX*	S288c	*this study*
yFA2165	*Δfes1::kanMX*	S288c	*this study*
yFA2169	*Δsnl1::kanMX*	S288c	*this study*
yFA1895	*Δsse1::hphNT2, Δapj1::NatNT2*	S288c	*this study*
yFA3562	*Δpdr5::NatNT2*	S288c	*this study*
yFA0371	*pre1-1::KanMX6*	S288c	*(Li et al., 2011)*
yFA2272	*pre1-1::KanMX6, Δapj1::NatNT2*	S288c	*this study*
yFA4616	*pre1-1::KanMX6, Δhsp104::KanMX6*	S288c	*this study*
yFA4617	*pre1-1::KanMX6, Δhsp104::KanMX6, Δapj1::NatNT2*	S288c	*this study*
yFA2476	*Δsan1::NatNT2*	S288c	*this study*
yFA2589	*Δapj1::hphNT2, Δsan1::NatNT2*	S288c	*this study*
yFA3613	*Δubr1::KanMX6*	S288c	*this study*
yFA2585	*Δapj1::hphNT2, Δubr1::NatNT2*	S288c	*this study*
yFA4701	*Δdoa10::LEU2MX6*	S288c	*this study*
yFA4702	*Δapj1::NatNT2, Δdoa10::KanMX6*	S288c	*this study*
yFA4618	*Δapj1, Δpdr5, Nup49-mars*	S288c	*this study*
yFA3520	*URA3::CMV-tTA, pSIS11::kanR-tet07-TATA*	S288c	*Open Biosystems*
yFA3524	URA3::CMV-tTA, Δapj1::NatNt2, pSIS11::kanR-tet07-TATA	S288c	*this study*
yFA4061	*Δxdj1::His3MX6*	S288c	*this study*
yFA1518	*Δcaj1::hphNT2*	S288c	*this study*
yFA4136	*Δdjp1::KanMX*	S288c	*this study*
yFA3519	*ydj1-2::His3, Leu2::ydj1-151, prc1-1*	W303	*(Park et al., 2007)*

yFA3554	*ydj1-2::His3, Leu2::ydj1-151, prc1-1, Δapj1::NatNt2*	W303	*this study*
yFA4693	Δsan1::NatNT2, Δubr1::KanMX6, Δdoa10::His3	S288c	*this study*
yFA4694	*Δsan1::NatNT2, Δubr1::KanMX6, Δdoa10::His3, Δapj1::Leu2MX6*	S288c	*this study*
yFA4699	*Δhsp104::hphNT2, Δubr1::KanmX6, Δsan1::NatNT2, Δdoa10::His3*	S288c	*this study*
yFA4700	*Δhsp104::hphNT2, Δubr1::KanmX6, Δsan1::NatNT2, Δapj1::His3, Δdoa10::LEU2MX6*	S288c	*this study*

Li, Z., F.J. Vizeacoumar, S. Bahr, J. Li, J. Warringer, F.S. Vizeacoumar, R. Min, B. Vandersluis, J. Bellay, M. Devit, J.A. Fleming, A. Stephens, J. Haase, Z.Y. Lin, A. Baryshnikova, H. Lu, Z. Yan, K. Jin, S. Barker, A. Datti, G. Giaever, C. Nislow, C. Bulawa, C.L. Myers, M. Costanzo, A.C. Gingras, Z. Zhang, A. Blomberg, K. Bloom, B. Andrews, and C. Boone. 2011. Systematic exploration of essential yeast gene function with temperature-sensitive mutants. *Nat. Biotechnol.* 29:361-367.

Park, S.H., N. Bolender, F. Eisele, Z. Kostova, J. Takeuchi, P. Coffino, and D.H. Wolf. 2007. The cytoplasmic Hsp70 chaperone machinery subjects misfolded and endoplasmic reticulum import-incompetent proteins to degradation via the ubiquitin-proteasome system. *Mol Biol Cell*. 18:153-165.